

Contribution of the Interdecadal Pacific Oscillation to twentieth-century global surface temperature trends

Gerald A. Meehl^{1*}, Aixue Hu¹, Benjamin D. Santer² and Shang-Ping Xie³

Longer-term externally forced trends in global mean surface temperatures (GMSTs) are embedded in the background noise of internally generated multidecadal variability¹. A key mode of internal variability is the Interdecadal Pacific Oscillation (IPO), which contributed to a reduced GMST trend during the early 2000s^{1–3}. We use a novel, physical phenomenon-based approach to quantify the contribution from a source of internally generated multidecadal variability—the IPO—to multidecadal GMST trends. Here we show that the largest IPO contributions occurred in its positive phase during the rapid warming periods from 1910–1941 and 1971–1995, with the IPO contributing 71% and 75%, respectively, to the difference between the median values of the externally forced trends and observed trends. The IPO transition from positive to negative in the late-1990s contributed 27% of the discrepancy between model median estimates of the forced part of the GMST trend and the observed trend from 1995 to 2013, with additional contributions that are probably due to internal variability outside of the Pacific⁴ and an externally forced response from small volcanic eruptions⁵. Understanding and quantifying the contribution of a specific source of internally generated variability—the IPO—to GMST trends is necessary to improve decadal climate prediction skill.

Several previous studies have addressed the issue of identifying internally generated contributions to GMST by starting with a multi-model average (MMA) estimate of the externally forced GMST response and subtracting this response from observations, thus yielding internally generated decadal variability as a residual. The GMST residuals ('noise') are assumed to represent the combined effects of all modes of internal variability, and an IPO-like surface temperature pattern has been shown to be associated with the decadal variability of GMST since 1920⁴. But use of a global empirical orthogonal function (EOF) analysis did not explicitly isolate the contribution of the IPO. An alternate approach for estimation of an IPO contribution involved specifying the observed time-evolving sea surface temperatures (SSTs) in the eastern tropical Pacific in a global coupled climate model². This simulation successfully replicated many key features of observed GMST changes, particularly the muted post-2000 surface warming trend⁶, suggesting that knowledge of the time evolution of the IPO could inform our understanding of multidecadal variability of GMST. Although external forcings were not explicitly varied, their influences were included in the prescribed SSTs^{2,7}—that is, variability in the prescribed SSTs does not solely reflect variability in the IPO.

These approaches do not improve understanding of the processes and mechanisms that contribute to the residual GMST variability. Furthermore, they do not consider the possibility of interaction between the forcing and internal variability⁸. Another problem lies with the assumption that the MMA provides the most reliable estimate of the forced response. Systematic errors in the MMA (for example, arising from the neglect of early twenty-first century volcanic forcing, incorrect representation of solar irradiance changes during the last solar cycle, possible underestimation of anthropogenic SO₂ emissions from China, and so on) are aliased in the observed GMST residuals. Thus, some component of the residual GMST variability is due to forcing errors, hampering reliable quantification of the IPO contribution. This difficulty is also a factor in techniques that use multivariate regression on spatio-temporal patterns of forced response and IPO variability to estimate the relative contributions of each factor to the time evolution of the GMST.

Here we take the novel approach of addressing the problem from the opposite direction. Rather than inferring 'total' internal variability as a residual, we start with an estimate of internally generated variability from a specific source—SSTs associated with the IPO in the Pacific from a long unforced climate model control run. We then compare the size of the IPO contribution to the observed time series of twentieth-century GMST, with the size of the contribution from the externally forced response (estimated from the multi-model average of simulations with combined anthropogenic and natural external forcings; see Methods in Supplementary Information).

In this Letter we are concerned with the influence of all causes of the interdecadal variability of Pacific SST on globally averaged surface temperature, which we summarize in the form of the IPO. We recognize (Supplementary Section 3) that the IPO concept may include aspects of the interdecadal modulation of high-frequency ENSO variability, but unravelling the detailed mechanisms is not essential to the validity of the conclusions we draw. A caveat is that systematic errors in model response could affect internally generated variability as well as the response to external forcings. A second caveat (as noted above in discussion of estimating total internal variability by subtraction) is that systematic errors in external forcings influence the size of simulated GMST changes, and thus impact inferences about the relative sizes of IPO and externally forced contributions.

The second EOF of low-pass-filtered observed SSTs is shown in Fig. 1b. Its principal component (PC) time series (Supplementary Fig. 7b) is typically taken to be an index of the IPO⁹. In Fig. 1c,

¹National Center for Atmospheric Research, Boulder, Colorado 80301, USA. ²Program for Climate Model Diagnosis and Intercomparison, Lawrence Livermore National Laboratory, Livermore, California 94550, USA. ³Scripps Institution of Oceanography, University of California San Diego, La Jolla, California 92037, USA. *e-mail: meehl@ucar.edu

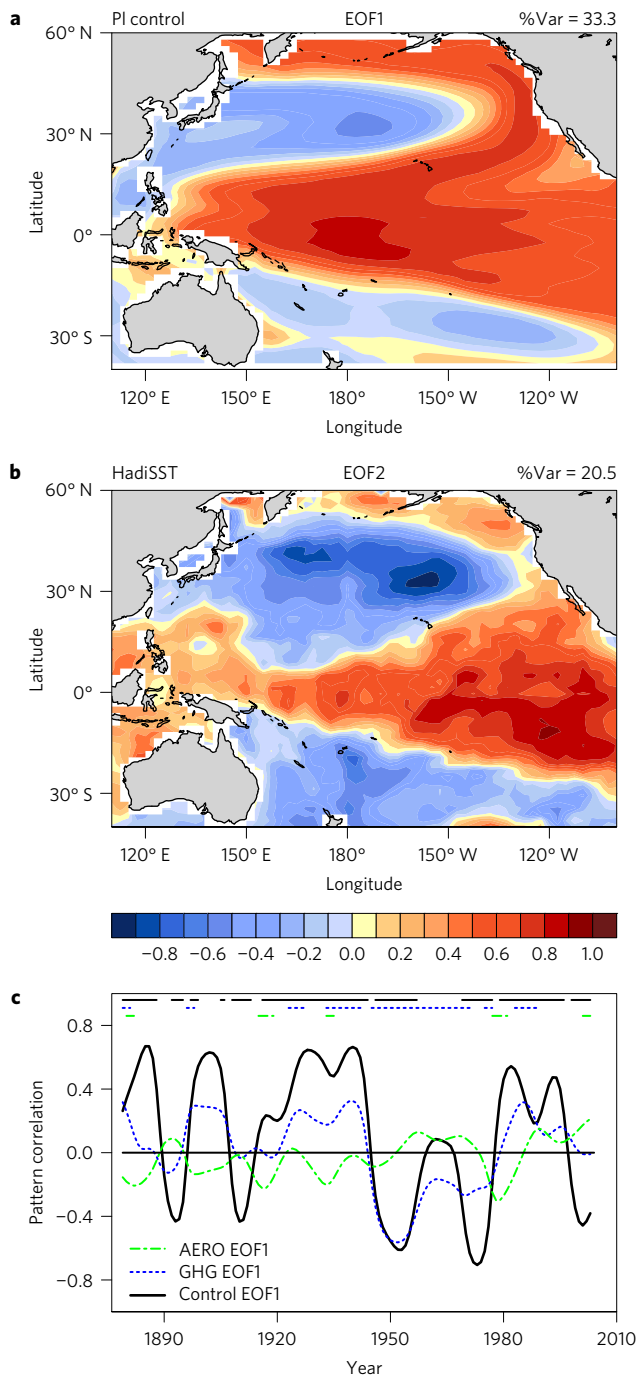


Figure 1 | Observed IPO compared to multi-model internally generated IPO and externally forced response from aerosols and greenhouse gases.

a, Multi-model average EOF1 pattern from the control runs (the models' IPO). **b**, Pattern of the observed IPO (see Supplementary Fig. 7). **c**, Pattern correlations from projecting the models' IPO pattern in **a** onto the time-varying low-pass-filtered observed SSTs (black line, comparable to observed IPO index in Supplementary Fig. 7b), and for the time-invariant multi-model average EOF1 from AERO (green dash-dot) and GHG (blue dotted) experiments (Supplementary Fig. 6) projected onto the observed SSTs. The significance of the pattern correlations from a Pearson R test are shown at the top: when a line is plotted, correlations are significant at the 5% level or better. %Var in **a** and **b** refers to the per cent variance that is explained by the EOF. The colour scale denotes correlation values.

the time-invariant EOF1 patterns from the multi-model ensemble mean AERO (sulfate aerosol only), GHG (greenhouse gas only),

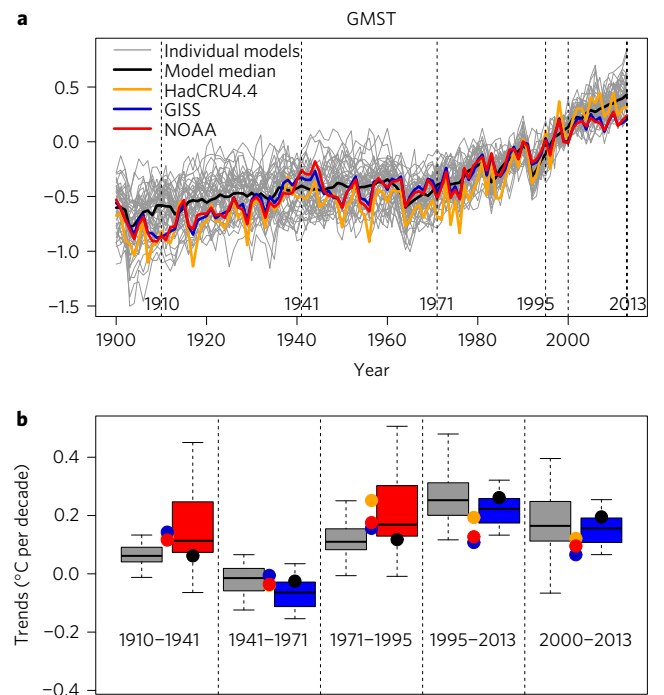


Figure 2 | IPO contributions to observed GMST trends. **a**, Annual mean observed GMST anomalies and individual ensemble members from the CMIP5 models (1986–2005 base period). **b**, Observed decadal trends (coloured dots, see legend in **a**) corresponding to positive or negative IPO epochs in **a**. The multi-model ensemble average forced response is shown by the black dots. The box plots show the distribution of GMST trends. The black lines are the median values, boxes are the 25th and 75th percentiles and whiskers indicate the 5th and 95th percentiles. The grey boxes denote externally forced trends; coloured boxes (red for positive IPO, blue for negative IPO) are for GMST trends adjusted from the corresponding externally forced GMST model trends to take into account the contributions from the distribution of positive and negative decadal IPO GMST trends computed from the CCSM4 control run.

and control runs (EOF1 pattern in Fig. 1a taken to be the internally generated IPO, pattern correlation with the observed IPO in Fig. 1b is +0.70; EOF1 patterns and PC time series for AERO and GHG are shown in Supplementary Fig. 6) are projected onto the time-varying low-pass-filtered observed SSTs. The model IPO (solid black line) is comparable to the time evolution of the observed IPO index (Supplementary Fig. 7b, correlation of +0.91), and has larger amplitude values in Fig. 1c than AERO and GHG. This confirms previous single model results⁹ in that the internally generated IPO from the models has the greatest correspondence to the observed IPO, and is the dominant contributor to the time-evolving patterns of observed low-frequency SST variability in the Pacific. AERO and GHG single forcings show generally smaller contributions. Section S5 in the Supplementary Information discusses the relationship between the pattern correlation calculations in Fig. 1 and the trends in the PC time series from the individual forcings in Supplementary Fig. 6.

Figure 2a compares the CMIP5 multi-model median (MMM) GMST changes with observed GMST anomalies over 1910 to 2013 (see Methods in Supplementary Information). The lengths of the simulated IPO epochs are defined based on the years when the index begins trending towards opposite sign epochs (Fig. 1c and Supplementary Fig. 7b, see Methods in Supplementary Information).

To quantify how much the IPO may have contributed to observed GMST trends over these specific periods of time (Fig. 2a), we choose a multi-century unforced control run (the last 1100 years from a 1300-year integration) from CCSM4. This model is appropriate here

because it has been analysed the most extensively of any current climate model with regards to IPO processes and mechanisms, and compares favourably in those aspects to observations^{10–12} and to the multi-model average IPO pattern in Fig. 1a (pattern correlation of +0.90). CCSM4 control run output was used to compute the distributions of unforced ten-year trends in globally averaged GMST. We considered only those GMST trends occurring at times of positive and negative ten-year trends in the model IPO (see Methods in Supplementary Information). The box and whisker plots in Fig. 2b show the result of accounting for CCSM4's estimate of the IPO influence on GMST trends when the IPO is trending positive (red boxes) or negative (blue boxes). By adding the IPO-mediated trend distributions inferred from the CCSM4 control run to the median trend calculated from the multi-model ensemble of CMIP5 simulations with historical forcing (representing the externally forced response, grey boxes), we form 'IPO-adjusted' distributions of GMST trends for each epoch. The observational trend results for each epoch are compared with both 'IPO-adjusted' and 'unadjusted' (externally forced) model GMST trends (see Methods in Supplementary Information).

We consider first the two epochs when the IPO is in its positive phase (1910–1941 and 1971–1995). During both observational periods with positive trends in the IPO, the distributions of the 'IPO-adjusted' model trend values shift upwards compared to the forced trend distributions. The 'adjusted' results are noticeably closer to the observed trend values (coloured dots) than the corresponding distributions of externally forced model trends (grey boxes). Additionally, the observational trends are closer to the median of the IPO-adjusted distributions (the solid black line in the red boxes) than to the median of the unadjusted trends (the solid black line in the grey boxes). In each of the 'positive IPO phase' epochs, all of the observational trends are within the 25–75% range for the IPO-adjusted values (red boxes), but not the externally forced trend distributions (grey boxes).

For the 1910–1941 period, the median of the observations is +0.13 °C per decade (range +0.12 to +0.14 °C per decade), the multi-model median of the unadjusted trends is +0.06 °C per decade (25–75% range of +0.04° to +0.09 °C per decade), and the IPO-adjusted median value is +0.11 °C per decade (+0.07° to +0.25 °C per decade). Thus, the IPO accounts for 71% of the discrepancy between the median values of the forced response and the observed GMST trends during this period. For the 1971–1995 period, the observed median value of +0.19 °C per decade (+0.16° to +0.25 °C per decade) is closer to the IPO-adjusted median value of +0.17 °C per decade (+0.13° to +0.30 °C per decade) than to the externally forced trend value of +0.11 °C per decade (+0.08° to +0.15 °C per decade). Thus, the IPO could account for 75% of the discrepancy between the median values of the forced response and the median of the observed GMST trends during this time period.

For the big hiatus period from 1941–1971, the IPO-adjusted median value produces a larger-than-observed trend of –0.06 °C per decade, compared with the multi-model forced value of –0.01 °C per decade and observed median value of –0.03 °C per decade. In this case, there is a slight over-correction in the adjustment for the negative phase of the IPO. However, the two pulses of negative IPO during the big hiatus (Fig. 1c) probably had contributions from a combination of internally generated variability from the IPO and external forcing (see Supplementary Information and Supplementary Fig. 1).

For the recent hiatus from 1995–2013, the median of the observed results of 0.14 °C per decade (+0.11° to +0.19 °C per decade) is closer to the median of the IPO-adjusted trend value of +0.22 °C per decade (+0.17° to +0.26 °C per decade) than to the median of the unadjusted results of +0.25 °C per decade (+0.20° to +0.31 °C per decade) (Fig. 2b). In this period, therefore, the CCSM4-based estimate of IPO variability can account for 27% of

the difference between the observed trends and the median of the unadjusted externally forced model trends. Similar results are obtained for a slightly different definition of the negative IPO period from 2000–2013 (Fig. 2b). We note that both the unadjusted and adjusted model results do not include the effects from a series of moderate volcanic eruptions in the early twenty-first century, and thus are likely to be biased warm^{5,13}. Accounting for these effects would probably bring both the unadjusted and adjusted multi-model median trends in Fig. 1b closer to the observed values^{5,7,14,15}. Thus, the results shown here indicate that discrepancies between simulated and observed trends over the early twenty-first century warming slowdown are likely to be attributable not only to the IPO, but also to volcanic (and other) external forcings, as well as to possible contributions from Atlantic SSTs associated with the Atlantic Multidecadal Oscillation⁴ (AMO, see Supplementary Information). Another factor is that the changing background base state, which is characterized by a long-term warming trend, would produce less of a contribution from the IPO to a slowdown in decadal GMST trends as the forcing from greenhouse gases continues to increase into the twenty-first century¹⁶. This was also noted in future climate simulations where the IPO influence on decadal GMST trends is reduced in scenarios with large greenhouse gas forcing compared to medium or lower forcing scenarios¹⁷. IPO variability also has been shown to influence trends in other parts of the climate system in addition to GMST, such as Antarctic sea ice expansion from 2000–2014 during the negative phase of the IPO¹⁸. Therefore, understanding and quantifying IPO contributions to climate variability in conjunction with the forced response (from factors such as increasing GHGs) will help improve decadal climate predictions¹⁹.

Received 12 April 2016; accepted 20 July 2016;
published online 29 August 2016

References

1. Fyfe, J. *et al.* Making sense of the early-2000s warming slowdown. *Nat. Clim. Change* **6**, 224–228 (2016).
2. Kosaka, Y. & Xie, S.-P. Recent global-warming hiatus tied to equatorial Pacific surface cooling. *Nature* **501**, 403–407 (2013).
3. Trenberth, K. E. Has there been a hiatus? *Science* **349**, 691–692 (2015).
4. Dai, A., Fyfe, J. C., Xie, S.-P. & Dai, X. Decadal modulation of global surface temperature by internal climate variability. *Nat. Clim. Change* **5**, 555–559 (2015).
5. Santer, B. D. *et al.* Volcanic contributions to decadal changes in tropospheric temperature. *Nat. Geosci.* **7**, 185–189 (2014).
6. Meehl, G. A., Teng, H. & Arblaster, J. M. Climate model simulations of the observed early-2000s hiatus of global warming. *Nat. Clim. Change* **4**, 898–902 (2014).
7. Santer, B. D. *et al.* Observed multivariable signals of late 20th and early 21st century volcanic activity. *Geophys. Res. Lett.* **42**, 500–509 (2015).
8. Maher, N., McGregor, S., England, M. H. & Sen Gupta, A. Effects of volcanism on tropical variability. *Geophys. Res. Lett.* **42**, 6024–6033 (2015).
9. Meehl, G. A., Hu, A. & Santer, B. D. The mid-1970s climate shift in the Pacific and the relative roles of forced versus inherent decadal variability. *J. Clim.* **22**, 780–792 (2009).
10. Meehl, G. A. *et al.* Model-based evidence of deep-ocean heat uptake during surface-temperature hiatus periods. *Nat. Clim. Change* **1**, 360–364 (2011).
11. Meehl, G. A., Hu, A., Arblaster, J. M., Fasullo, J. & Trenberth, K. E. Externally forced and internally generated decadal climate variability associated with the Interdecadal Pacific Oscillation. *J. Clim.* **26**, 7298–7310 (2013).
12. Meehl, G. A. & Teng, H. Case studies for initialized decadal hindcasts and predictions for the Pacific region. *Geophys. Res. Lett.* **39**, L22705 (2012).
13. Solomon, S. *et al.* The persistently variable "background" stratospheric aerosol layer and global climate change. *Science* **333**, 866–870 (2011).
14. Ridley, D. A. *et al.* Total volcanic stratospheric aerosol optical depths and implications for global climate change. *Geophys. Res. Lett.* **41**, 7763–7769 (2014).
15. Andersson, S. M. *et al.* Significant radiative impact of volcanic aerosol in the lowermost stratosphere. *Nat. Commun.* **6**, 7692 (2015).
16. Watanabe, M. *et al.* Contribution of natural decadal variability to global warming acceleration and hiatus. *Nat. Clim. Change* **4**, 893–897 (2014).

17. Maher, N., Sen Gupta, A. & England, M. H. Drivers of decadal hiatus periods in the 20th and 21st centuries. *Geophys. Res. Lett.* **41**, 5978–5986 (2014).
18. Meehl, G. A., Arblaster, J. M., Bitz, C., Chung, C. T. Y. & Teng, H. Antarctic sea ice expansion between 2000–2014 driven by tropical Pacific decadal climate variability. *Nat. Geosci.* **9**, 590–595 (2016).
19. Meehl, G. A., Hu, A. & Teng, H. Initialized decadal prediction for transition to positive phase of the Interdecadal Pacific Oscillation. *Nat. Commun.* **7**, 11718 (2016).

Acknowledgements

The authors thank C. Tebaldi for her contributions to formulating the GMST trend distributions and for stimulating discussions on how to quantify the relative roles of internal variability and externally forced response, and G. Jones for providing the masked CMIP5 model data. Portions of this study were supported by the Regional and Global Climate Modeling Program (RGCM) of the US Department of Energy's Office of Biological & Environmental Research (BER) Cooperative Agreement # DE-FC02-97ER62402 and the National Science Foundation. We acknowledge the World Climate Research Programme's Working Group on Coupled Modelling, which is responsible for CMIP, and we thank the climate modelling groups for producing and

making available their model output. For CMIP, the US Department of Energy's Program for Climate Model Diagnosis and Intercomparison provides coordinating support and led development of software infrastructure in partnership with the Global Organization for Earth System Science Portals. The National Center for Atmospheric Research is sponsored by the National Science Foundation.

Author contributions

G.A.M. directed this work with contributions from all authors. G.A.M., A.H. and B.D.S. contributed to model data analysis. G.A.M., A.H., B.D.S. and S.-P.X. contributed to writing the paper. All authors discussed the results and commented on the manuscript.

Additional information

Supplementary information is available in the [online version of the paper](#). Reprints and permissions information is available online at www.nature.com/reprints. Correspondence and requests for materials should be addressed to G.A.M.

Competing financial interests

The authors declare no competing financial interests.